Investigo
Universidade Vigo

Biblioteca Universitaria
Área de Repositorio Institucional

Tfno.: 986 813 821
investigo@uvigo.gal

This document is the Accepted Manuscript version of a Published Work that appeared in final form in *Organic Letters*, copyright © 2019 American Chemical Society after peer review and technical editing by the publisher. To access the final edited and published work see: https://doi.org/10.1021/acs.orglett.9b02024

Cite this:

Double Protonation of a cis-Bipyridoallenophane Detected via Chiral-Sensing Switch: The Role of Ion Pairs.

Silvia Castro-Fernández, Jonathan Álvarez-García, Luís García-Río, Carlos Silva-López, and María Magdalena Cid. *Organic Letters* 2019 21 (15), 5898-5902, DOI: 10.1021/acs.orglett.9b02024

Double-protonation of a *cis*-Bipyridoallenophane detected via chiral-sensing Switch: Role of Ion-Pairs

Silvia Castro-Fernández[‡a] Jonathan Álvarez-García, [‡a] Luís García-Río,[b] Carlos Silva-López[a] and María Magdalena Cid*[a]

[a]*Departamento de Química Orgánica, Edificio Ciencias Experimentais, Campus Lagoas-Marcosende, Vigo, E-36310 Spain.*

[b]*Centro Singular de Investigación en Química Biolóxica e Materiais Moleculares (CIQUS), Departamento de Química Física, Universidade de Santiago de Compostela, 15782 Santiago de Compostela (Spain).*

Supporting Information Placeholder

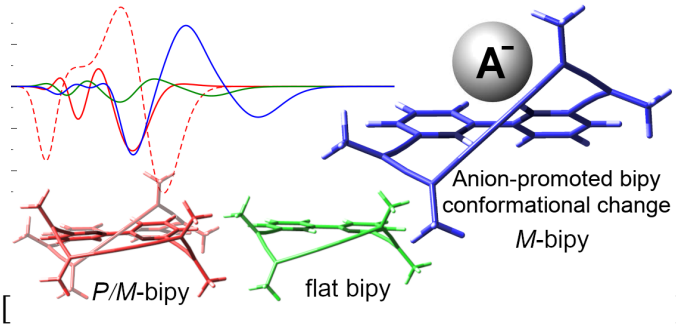

[ ]

ABSTRACT: We proved that the confinement of the conformational space of pyridoallenophanes leads to intense chiroptical responses. Unlike the cyclic dimer [14_2], single-conformation [14_1]pyridoallenophanes isomerized under thermal and photochemical conditions. Yet, less-strained [14_1]bipyridoallenophanes were stable and prepared successfully. They, unexpectedly, underwent double protonation as result of cooperative ion-pairing and hydrogen bonding. The complex formation forced a single-configuration of the axis connecting both pyridyl rings recognized by a diagnostic circular-dichroism signal at 330 nm.

Chiral macrocyclic systems have shown broad applicability as molecular receptors.[1,2] The high sensitivity of chiroptical responses to conformational changes[3-5] and intermolecular interactions would furnish chiral shape-persistent macrocycles[2,6,7] with outstanding sensing capabilities.[8-10] In this regard, the use of systems with narrow conformational space is desired in order to maximize chiroptical response intensities.[11,12] We therefore considered allenophanes as good candidates to build highly responsive chiral macrocycles since allenes offer both requirements: chirality and conformational rigidity. During the last years, diethynylallenes (DEAs) along with aromatic connectors have already been used to create structures with different shapes, sizes, and functionalities.[13-18] We have reported the preparation and full characterization of [14_2]-meta-allenophane **1** whose conformational space is described by three possible conformers[19] of which only two coexist in solution (Figure 1).[20] A further step to improve the capabilities of these compounds would be to achieve single-conformation chiral allenophanes in order to obtain strong chiroptical responses upon non-covalent chiral recognition.[21,22] Thus, to increase the confinement of the conformational space, we decided to move from $(DEA)_4$ to smaller allenic macrocycles $(DEA)_2$ as in **2** and **3**.

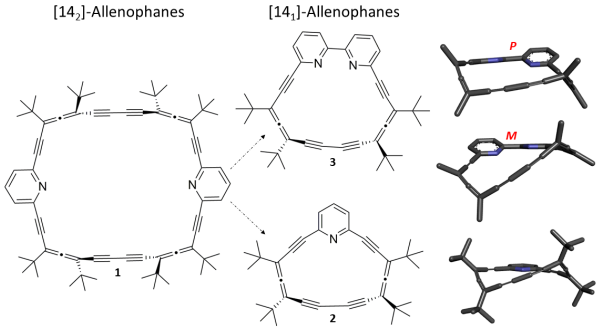

Figure 1. [14_2]-Pyridoallenophane **1** and [14_1]-pyrido- and bipyridoallenophanes, **2** and **3,** along with the corresponding conformers (DFT CAM-B3LYP/6-31G+(d,p))

Here we present the synthesis and structural characterization of enantiopure $(DEA)_2$-allenophanes, maintaining the meta arrangement on the aromatic connector. The unit $(DEA)_2$ was closed using pyridine and bipyridine rings, as in **2** and **3**, both very versatile sensing/coordinating motifs.[23,24] The inherent twist of a locked *cis*-bipyridine should provide shape-persistent macrocyclic systems with adaptability to facilitate bind-

ing interactions.[25] Here we demonstrate that chiral *cis*-bipyridoallenophanes undergo a switch in its expression of chirality upon protonation and ion-pair binding.

Allenophane (*M*,*M*)-**2**, initially obtained as a side product in the synthesis of (*M*,*M*,*M*,*M*)-**1**, was prepared, in 18% overall yield from DEA, facilitating the intramolecular cyclization by raising the reaction temperature (see SI Table S1, Figures S8-S9). This compound showed only one conformer and an outstanding chiroptical response with a maximum dissymmetry factor[26] ($\Delta\varepsilon/\varepsilon$) g = 0.011, which is almost twice that of the **[14$_2$]** analogue **1** (0.006), even though we have reduced by half the number of chiral units (see Figure 2a). Unexpectedly, enantiopure **2** underwent *P*/*M*-isomerization processes under thermal and photochemical conditions as evidenced by CD intensities vanishing with time preventing further use (see Figure S7B). This observation was unforeseen since isomerization processes had previously been observed in allenes conjugated with electron-donor groups, unlike pyridine.[16,27] DFT calculations (CAM-B3LYP/6-31+G(d,p)) resulted in a barrier of 27.5 kcal/mol for thermal *M*-*P* isomerization of one allene fragment in **2**; a similar value was found for the photochemically driven isomerization (see SI for details). This activation barrier value is compatible with a relatively fast process at room temperature.[28]

We assumed initially that the governing factor for the isomerization of **2** was mainly ring strain. We therefore hypothesized that, by substituting the pyridine ring in **2** with a bipyridine fragment such as in allenophane **3**, some of this strain would be reduced.

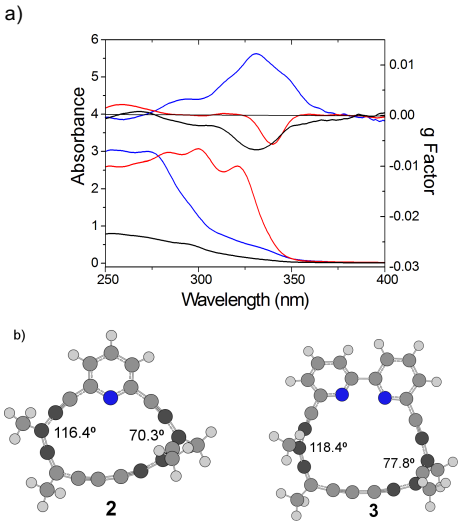

Figure 2. a) UV spectra (bottom) and *g*-factor representations (top) of (*P*,*P*,*P*,*P*)-**1** (red), (*M*,*M*)-**2** (blue) and (*P*,*P*)-**3** (black); b) geometries and key structural parameters computed for **2** and **3** at CAM-B3LYP/6-31+G(d,p) level of theory (atoms used to measure bond and dihedral angles shown in darker grey).

In good agreement with this postulation, the calculated *P*/*M*-isomerization activation barrier for **3** increased to 32.1 kcal/mol. A comparison between the computed geometries of **2** and **3** reveals that ring strain is indeed alleviated in the second. The dihedral angles between the allenes at these structures are 70.3 and 77.8° for **2** and **3**, respectively, evidencing that the allene fragments in the second are less distorted; bond angles (116.4 and 118.4°) follow the same trend (Figure 2 b).

Calculation of isodesmic processes however rendered almost equal energies for both **2** and **3** (Figures S35 and S36) suggesting that the ring strain only affects the kinetics of the isomerization process, not the relative stability of the final macrocycle.[29]

Thus, following the methodology developed in our group,[13,14] **3** was prepared in 62% overall yield from DEA vía **4**, which underwent an alkyne homocoupling process under Breslow conditions at room temperature once the protecting groups were removed (Scheme 1). (*P*,*P*)-**3** showed a high chiroptical response with a *g*-factor value of 0.007 with no loss of CD intensity under ambient conditions (Figure 2a).

Scheme 1. Synthesis of allenophanes 3

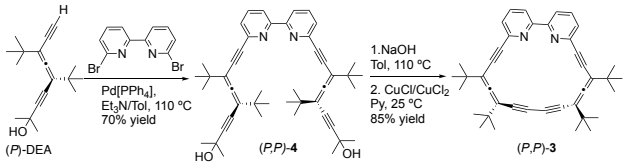

With chiral bipyridine (*P*,*P*)-**3** at hand, we were set out to test its chiroptical response upon proton sensing. Thus, by addition of TFA, a UV-band at 375 nm gradually appeared and so did a negative Cotton effect in (*P*,*P*)-**3** ECD spectra in chloroform. The presence of isosbestic points both in the ECD and the UV spectra, at first, pointed to an equilibrium between protonated (*P*,*P*)-**3•H** and unprotonated (*P*,*P*)-**3** species.[#30] Nevertheless, the titration curve did not present the typical logarithmic shape for a single equilibrium process. Indeed**,** the data resulted to perfectly fit with a double protonation process with oddly similar association constant values for the first and second protonation (K_1 = 104 ± 7 M^{-1} and K_2 = 95 ± 6 M^{-1}).[$] This is, to our knowledge, one of the few reports on a double protonation of a *cis*-bipyridine.[31,32] The ease of double protonation of **3** evokes its hydrogen bond-driven co-crystallization with two molecules of chloroform (Figures 3 left and S19).

In order to clarify this behavior, the titration of (*P*,*P*)-**3** was run with a stronger acid, TfOH in CH_3CN (The pK_a of TfOH in acetonitrile is reported to be 2.6 ± 0.1[33]). In this case, we were surprised by the emergence of a first saturation point well below stoichiometry for a one-protonation process (green line in Figure 3 right).

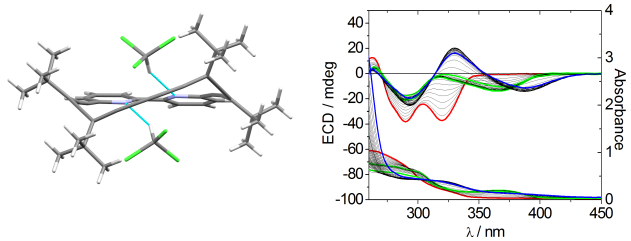

Figure 3. Left, crystal structure of (*P*,*P*)-**3** showing a M configuration of the bipyridine moiety; right, titration course of **3** with TfOH in CH_3CN: red lines represent the initial ECD (top) and UV (bottom) spectral bands and green/blue lines represent spectral bands at saturation points .

Upon the addition of higher amounts of TfOH, the initial band appearing at 360 nm in the UV-Vis spectrum blue shifted to 330 nm reflecting diminished π-delocalization, whereas the corresponding band in the ECD spectrum moved to 388 nm (Figure 3 right) at the same time that a new band at 330 nm appeared, pointing to a major conformational change.[#]

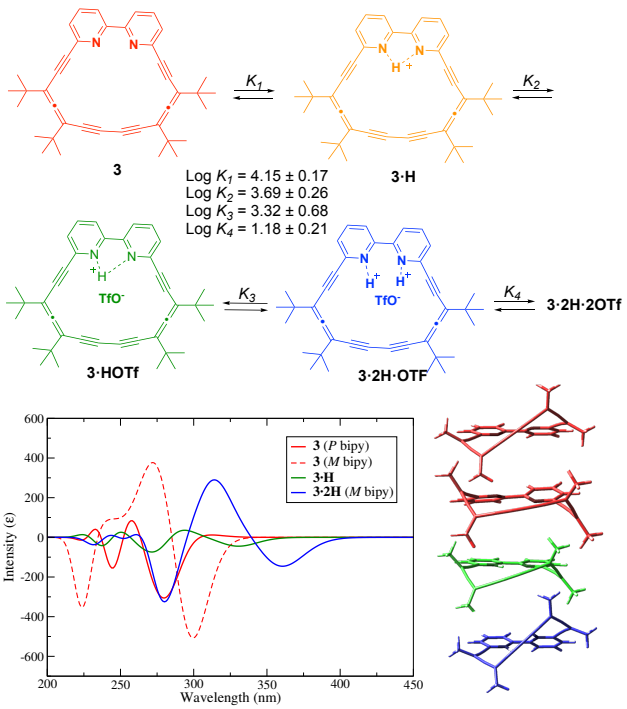

Figure 4. Top) proposed scheme for titration process for (*P*,*P*)-**3** with TfOH in CH_3CN; bottom) calculated CD for the most stable conformations of **3, 3·H** and **3·2H** (DFT CAM-B3LYP/6-31G+(d,p).

The experimental results obtained in the presence and in the absence of 0.138 M of TfO^- (to reflect the acid homoconjugation effect, see Figure 5) could be mathematically adjusted to multiple equilibria using ReactLab™ Equilibria software only when the concurrence of ion-pairs was taken into account[34-36] (full data in Tables S3-S4 and Figures S28-30). In doing so, the results showed that there is a facile first protonation with $K \approx 10^4$ M^{-1} and revealed one striking observation: free base **3** is still present at the time the diprotonated species, **3•2H**, starts to appear. The computed CD spectra of both conformations at the bipyridine fragment in **3•2H OTf** suggest that the conformer in solution exhibits a M configuration at this heterocyclic linker (a diagnostic positive Cotton effect at 310 nm was used coinciding remarkably well with the experimental one at 330 nm) while **3** seems to have not a preferred configuration in solution (see solid red line in Figure 3 right and red lines in Figure 4 bottom, experimental and calculated CD of **3**, respectively).

In order to confirm these results, titrations with TfOH monitored by NMR were performed. ^1H and ^{13}C NMR confirmed that several fast equilibria are reached below 1:1 stoichiometry as already found in the CD study (both methods have rendered *Ka* values within experimental error; see Table S5, Figures S31-32 for details). ^1H NMR spectra showed easily exchangeable hydrogens separating three main set of signals, indicating the presence of at least two main types of acidic H, namely, **3•H** from 0.5-20 equiv. and **3·2H** from 50 equiv. onwards, being H_b the one that displays the biggest shift[37] (Figures 5 top and S31). Along the titration, H_b-triplet becomes a complex multiplet as consequence of the co-existence of species with quite different H_b and the higher similarity of the doublets H_a and H_c at the end of the titration is an indication of a greater bipyridine dihedral angle.

To decipher the role of the triflate anion, ^{19}F NMR spectra of TfOH/CH_3CN mixtures in the absence and presence of macrocycle **3** are reported in Figure 5. A well-known biphasic pattern due to TfOH dissociation shielding and anion homoconjugation deshielding effects is observed as a consequence of the emergence of TfO^- and $TfO^{-}\cdots H\cdots OTf$ species, respectively.[33] The comparison of both profiles shows clear qualitative and quantitative differences. In the presence of the macrocycle the upfield effect presents two discontinuities at ca. 1 and 5 equiv., indicative of the participation of, at least, two extra fluor-containing species, **3•H OTf** and **3•2H OTf**. A downfield effect is observed both in the absence and presence of macrocycle due to TfO^- homoconjugation. It is remarkable the effect of the macrocycle promoting the homoconjugation (downfield effect from 50 to 20 equiv.) because macrocycle mono- and bis-protonation increase [TfO^-] at lower TfOH concentrations[⊥].

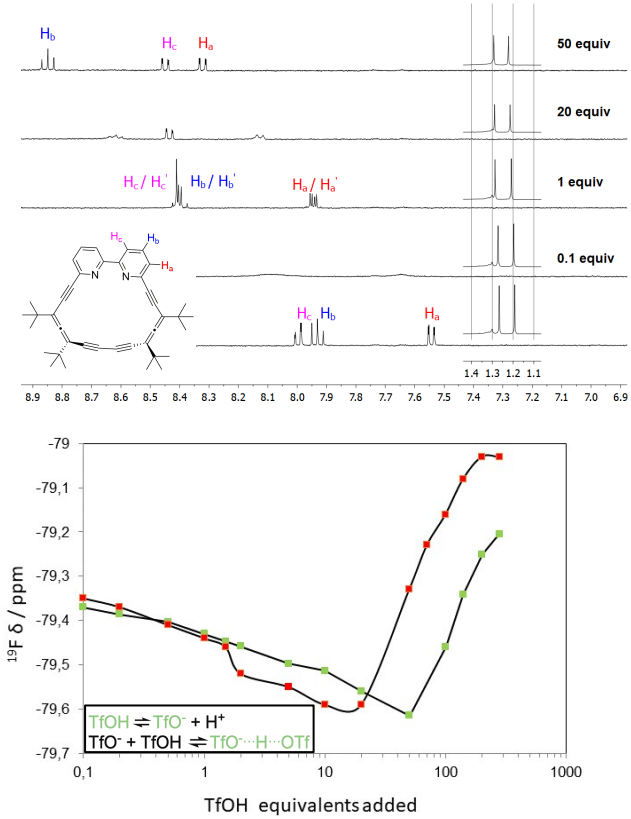

Figure 5. Allenophane **3** titration with TfOH in CD_3CN (from 0.1 to 280 equiv), top: aromatic region of selected ^1H NMR spectra; bottom: ^{19}F NMR, at 20 °C of TfOH in CD_3CN in the absence and presence of **3** (green and red points, respectively); inset: homoconjugation equilibria of TfOH in acetonitrile.

The prevalence of the bisprotonated species both with TFA and TfOH was proposed on the basis of a positive cooperativity involving an ion-pair binding between the monoprotonated macrocycle **3•H** with the non-dissociated acid form of TFA or TfOH.[36] The spatial arrangement of the anions fits into the macrocycle hollow in such a way hydrogen atoms would be shared by (*P*,*P*)-**3** and the oxoanions (TFA^- and TfO^-) as shown in the theoretically optimized geometries at Figure 6. The calculated structures of **3•2H TFA** and **3•2H OTf** show the bipyridine ring oriented towards the face of the ring hosting the anion and adopting a higher torsion angle (~40°) than

the free base (*P*,*P*)-**3** (~ –30°) between the two pyridine rings. The bond distances NH···O are 1.48 and 1.66 Å for TFA and TfO, respectively

Figure 6. Calculated geometry for **3•2H TFA**, left) and **3•2H OTf,** right at DFT-CAMB3LYP 6-31-G+(d,p) level of theory.

This intrinsic flexibility facilitates the electrostatic interactions. Thus, the ion-pair binding results from both hydrogen bonding and electrostatic interactions enhanced within the hydrophobic hollow of allenophane **3**.

In summary, we have demonstrated that shape-persistent allenophanes **2** and **3** display outstanding chiroptical responses (*g*-factor of 0.011 and 0.007, respectively). We have also shown that ring strain, unexpectedly, made **2** prone to undergo both thermal and photochemically driven isomerization processes. The torsion angle between both pyridine rings in **3** allows a double protonation to occur expedited by a stereoselective ion-pair binding. To the best of our knowledge, it is an exceptional occurrence for a *cis-locked*-bipyridine derivative. (*P*,*P*)-**3** accommodates the organic anions forming a close ion-pair within a chiral arrangement as shown by the appearance of a selective dichroic band in circular dichroism spectra due to a conformation switch.

ASSOCIATED CONTENT

Supporting Information

The Supporting Information is available free of charge on the ACS Publications website**.** Experimental procedures, spectroscopic characterization, theoretical calculations (pdf)**.**

AUTHOR INFORMATION

Corresponding Author

* E-mail: mcid@uvigo.es

ACKNOWLEDGMENTS

Financial support from Ministerio de Economia y Competitividad of Spain (CTQ2017-84354-P, CTQ2017-85919-R), Xunta de Galicia (ED431C 2017/70, IN607C 2016/03 and Centro singular de investigación de Galicia acreditation 2016-2019, ED431G/09) and the EU (European Regional Development Fund–ERDF) is gratefully acknowledged. Authors would like to thank the use of RIAIDT-USC analytical facilities.

REFERENCES

‡ Both authors contributed equally.

$ The spectral changes upon protonation were consistent with (TD)-DFT-based theoretical spectra (PCM-B3LYP/6-31+G(d,p) (CH_2Cl_2)) of the optimized structures **3·H** and **3·2H**, respectively (See Figures S20-S24).

Full reversibility was evidenced upon addition of triethylamine (Figures S20 and S25). Mirror images were obtained for (*M*,*M*)-**3** (see Figures S25-27).

⊥ Note that equilibrium constants K_2 and K_3 are very close while that for sequestering two triflate anions, K_4, is much lower.

(1) Zhang, X. X.; Bradshaw, J. S.; Izatt, R. M. Enantiomeric Recognition of Amine Compounds by Chiral Macrocyclic Receptors. *Chem. Rev.* **1997**, *97*, 3313–3362.

(2) Liu, Z.; Nalluri, S. K. M.; Stoddart, J. F. Surveying Macrocyclic Chemistry: From Flexible Crown Ethers to Rigid Cyclophanes. *Chem. Soc. Rev.* **2017**, *46*, 2459–2478.

(3) Rivera-Fuentes, P.; Alonso-Gómez, J. L.; Petrovic, A. G.; Santoro, F.; Harada, N.; Berova, N.; Diederich, F. Amplification of Chirality in Monodisperse, Enantiopure Alleno-Acetylenic Oligomers. *Angew. Chem. Int. Ed.* **2010**, *49*, 2247–2250.

(4) Donckele, E. J.; Gidron, O.; Trapp, N.; Diederich, F. Outstanding Chiroptical Properties: a Signature of Enantiomerically Pure Alleno-Acetylenic Macrocycles and Monodisperse Acyclic Oligomers. *Chem. Eur. J.* **2014**, *20*, 9558–9566.

(5) Pescitelli, G.; Di Bari, L.; Berova, N. Conformational Aspects in the Studies of Organic Compounds by Electronic Circular Dichroism. *Chem. Soc. Rev.* **2011**, *40*, 4603–4623.

(6) Kwit, M.; Grajewski, J.; Skowronek, P.; Zgorzelak, M.; Gawroński, J. One-Step Construction of the Shape Persistent, Chiral but Symmetrical Polyimine Macrocycles. *Chem Rec* **2019**, *19*, 213–237.

(7) Katoono, R.; Kawai, H.; Fujiwara, K.; Suzuki, T. Stereospecific Change in Conformation Upon Complexation of an Exoditopic Tetraamide Host with a Bis(Ammonium) Guest: Chiral Recognition and Strong CD Signaling. *Chem. Commun.* **2005**, 5154–5156.

(8) Pescitelli, G.; Di Bari, L.; Berova, N. Application of Electronic Circular Dichroism in the Study of Supramolecular Systems. *Chem. Soc. Rev.* **2014**, *43*, 5211–5233.

(9) Míguez-Lago, S.; Cid, M. M. Axially Chiral Shape-Persistent Encapsulating Agents. *Synthesis* **2017**, *49*, 4111–4123.

(10) Katoono, R.; Kusaka, K.; Saito, Y.; Sakamoto, K.; Suzuki, T. Chiral Diversification Through the Assembly of Achiral Phenylacetylene Macrocycles with a Two-Fold Bridge. *Chemical Science* **2019**, *10*, 4782–4791.

(11) Alonso-Gómez, J. L.; Rivera-Fuentes, P.; Harada, N.; Berova, N.; Diederich, F. An Enantiomerically Pure Alleno-Acetylenic Macrocycle: Synthesis and Rationalization of Its Outstanding Chiroptical Response. *Angew. Chem. Int. Ed.* **2009**, *48*, 5545–5548.

(12) Gidron, O.; Jirásek, M.; Wörle, M.; Diederich, F. Enantiopure Alleno-Acetylenic Helicages Containing Multiple Binding Sites. *Chem. Eur. J.* **2016**, *22*, 16172–16177.

(13) Lahoz, I. R.; Navarro-Vázquez, A.; Alonso-Gómez, J. L.; Cid, M. M. Acetylenic Homocoupling Methodology Towards the Synthesis of 1,3-Butadiynyl Macrocycles: [14_2]-Alleno-Acetylenic Cyclophanes. *Eur. J. Org. Chem.* **2014**, *2014*, 1915–1924.

(14) Lahoz, I. R.; Castro-Fernandez, S.; Navarro-Vázquez, A.; Alonso-Gómez, J. L.; Cid, M. M. Conformational Stable Alleno-Acetylenic Cyclophanes Bearing Chiral Axes. *Chirality* **2014**, *26*, 563–573.

(15) Castro-Fernandez, S.; Lahoz, I. R.; Llamas-Saiz, A. L.; Alonso-Gómez, J. L.; Cid, M. M.; Navarro-Vázquez, A. Preparation and Characterization of a Halogen-Bonded Shape-Persistent Chiral Alleno-Acetylenic Inclusion Complex. *Org. Lett.* **2014**, *16*, 1136–1139.

(16) Odermatt, S.; Alonso-Gómez, J. L.; Seiler, P.; Cid, M. M.; Diederich, F. Shape-Persistent Chiral Alleno-Acetylenic Macrocycles and Cyclophanes by Acetylenic Scaffolding with 1,3-Diethynylallenes. *Angew. Chem. Int. Ed. Engl.* **2005**, *44*, 5074–5078.

(17) Alonso-Gómez, J. L.; Navarro-Vázquez, A.; Cid, M. M. Chiral (2,5)Pyrido[7 4]Allenoacetylenic Cyclophanes: Synthesis and Characterization. *Chem. Eur. J.* **2009**, *15*, 6495–6503.

(18) Rivera-Fuentes, P.; Diederich, F. Allenes in Molecular Materials. *Angew. Chem. Int. Ed.* **2012**, *51*, 2818–2828.

(19) Lahoz, I. R.; Navarro-Vázquez, A.; Llamas-Saiz, A. L.; Alonso-Gómez, J. L.; Cid, M. M. Rotation-Locked 2,6-Pyrido-Allenophanes: Characterization of All Stereoisomers. *Chem. Eur. J.* **2012**, *18*, 13836–13843.

(20) Padula, D.; Lahoz, I. R.; Diaz, C.; Hernández, F. E.; Di Bari, L.; Rizzo, A.; Santoro, F.; Cid, M. M. A Combined Experimental-Computational Investigation to Uncover the Puzzling (Chiro-)Optical Response of Pyridocyclophanes: One- and Two-Photon Spectra. *Chem. Eur. J.* **2015**, *21*, 12136–12147.

(21) Wolf, C.; Bentley, K. W. Chirality Sensing Using Stereodynamic Probes with Distinct Electronic Circular Dichroism Output. *Chem. Soc. Rev.* **2013**, *42*, 5408.

(22) Forman, J. E.; Barrans, R. E.; Dougherty, D. A. Circular Dichroism Studies of Molecular Recognition with Cyclophane Hosts in Aqueous Media. *J. Am. Chem. Soc.* **1995**, *117*, 9213–9228.

(23) Ishida, M.; Naruta, Y.; Tani, F. A Porphyrin-Related Macrocycle with an Embedded 1,10-Phenanthroline Moiety: Fluorescent Magnesium(II) Ion Sensor. *Angew. Chem. Int. Ed.* **2010**, *49*, 91–94.

(24) Hapke, M.; Brandt, L.; Lützen, A. Versatile Tools in the Construction of Substituted 2,2′-Bipyridines—Cross-Coupling Reactions with Tin, Zinc and Boron Compounds. *Chem. Soc. Rev.* **2008**, *37*, 2782.

(25) Zahn, S.; Reckien, W.; Kirchner, B.; Staats, H.; Matthey, J.; Lützen, A. Towards Allosteric Receptors: Adjustment of the Rotation Barrier of 2,2′-Bipyridine Derivatives. *Chem. Eur. J.* **2009**, *15*, 2572–2580.

(26) Tanaka, H.; Ikenosako, M.; Kato, Y.; Fujiki, M.; Inoue, Y.; Mori, T. Symmetry-Based Rational Design for Boosting Chiroptical Responses. *Communications Chem.* **2018**, 1–8.

(27) Alonso-Gómez, J. L.; Schanen, P.; Rivera-Fuentes, P.; Seiler, P.; Diederich, F. 1,3-Diethynylallenes (DEAs): Enantioselective Synthesis, Absolute Configuration, and Chiral Induction in 1,1,4,4-Tetracyanobuta-1,3-Dienes (TCBDs). *Chem. Eur. J.* **2008**, *14*, 10564–10568.

(28) Silva López, C.; Alvarez, R.; Domínguez, M.; Nieto Faza, O.; de Lera, A. R. Complex Thermal Behavior of 11-*Cis*-Retinal, the Ligand of the Visual Pigments. *J. Org. Chem* **2009**, *74* (3), 1007–1013.

(29) López, C. S.; Faza, O. N.; Freindorf, M.; Kraka, E.; Cremer, D. Solving the Pericyclic-Pseudopericyclic Puzzle in the Ring-Closure Reactions of 1,2,4,6-Heptatetraene Derivatives. *J. Org. Chem.* **2016**, *81*, 404–414.

(30) James, P. V.; Yoosaf, K.; Kumar, J.; Thomas, K. G.; Listorti, A.; Accorsi, G.; Armaroli, N. Tunable Photophysical Properties of Phenyleneethynylene Based Bipyridine Ligands. *Photochem. Photobiol. Sci.* **2009**, *8*, 1432–1440.

(31) Thummel, R. P.; Lefoulon, F. Polyaza Cavity Shaped Molecules. 5. Annelated Derivatives of 2, 2'-Bipyridine. *J. Org. Chem.* **1985**, *50*, 3824–3828.

(32) Oresmaa, L.; Haukka, M.; Vainiotalo, P.; Pakkanen, T. A. Ab Initio Calculations and Mass Spectrometric Determination of the Gas-Phase Proton Affinities of 4,4′-Disubstituted 2,2′-Bipyridines. *J. Org. Chem.* **2002**, *67*, 8216–8219.

(33) Fujinaga, T.; Sakamoto, I. Electrochemical Studies of Sulfonates in Non-Aqueous Solvents: Part III. Trifluoromethanesulfonic Acid as a Strong Acid in Dipolar Aprotic Solvents and Acetic Acid. *Journal of Electroanalytical Chemistry and ...* **1977**, *85* (1), 185–201.

(34) Fuoss, R. M. Ionic Association. III. the Equilibrium Between Ion Pairs and Free Ions. *J. Am. Chem. Soc.* **1958**, *80*, 5059–5061.

(35) Qiao, B.; Sengupta, A.; Liu, Y.; McDonald, K. P.; Pink, M.; Anderson, J. R.; Raghavachari, K.; Flood, A. H. Electrostatic and Allosteric Cooperativity in Ion-Pair Binding: a Quantitative and Coupled Experiment–Theory Study with Aryl–Triazole–Ether Macrocycles. *J. Am. Chem. Soc.* **2015**, *137*, 9746–9757.

(36) Roelens, S.; Vacca, A.; Venturi, C. Binding of Ionic Species: A General Approach to Measuring Binding Constants and Assessing Affinities. *Chem. Eur. J.* **2009**, *15*, 2635–2644.

(37) Alkorta, I.; Elguero, J.; Roussel, C. A Theoretical Study of the Conformation, Basicity and NMR Properties of 2,2′-, 3,3′- and 4,4′-Bipyridines and Their Conjugated Acids. *Comp. Theo. Chem.* **2011**, *966*, 334–339.